Int. J. Heat Mass Transfer. Vol. 30, No. 4, pp. 781–789, 1987
Printed in Great Britain

0017–9310/87 $3.00 + 0.00

Measurements of mass transfer coefficient and effectiveness in the recovery region of a film-cooled surface†

W. P. WEBSTER
DOE-METC, Morgantown, WV 26505, U.S.A.

and

S. YAVUZKURT
Department of Mechanical Engineering, Pennsylvania State University, University Park, PA 16802, U.S.A.

(*Received* 19 *February* 1986 *and in final form* 12 *August* 1986)

Abstract—Mass transfer coefficients and film cooling effectiveness are measured downstream of a single row of holes (recovery region) inclined 30° with the surface and inline with the main turbulent boundary layer flow. The mass transfer coefficients are measured using a naphthalene sublimation technique. The effectiveness is determined through the injection of a trace gas into the secondary flow and measuring its concentration at the impermeable wall. Experiments are carried out in a subsonic, zero pressure gradient turbulent boundary layer, under isothermal conditions with three blowing ratios (U_j/U_∞): 0.4, 0.8, and 1.2. The data is collected in a region 7–80 jet diameters downstream of the injection location. From the data on mass transfer coefficients and effectiveness obtained under the same flow conditions a general mass transfer equation is derived. This paper presents extensive data and discussions; and is believed to be one of the few studies in which both of these variables are measured on the same surface and in a large area in the recovery region.

INTRODUCTION

GAS TURBINE blades have been shown to corrode due to the condensation of sulfides on the cooled blade surface [1]. These sulfides are formed when the sulfur in the fuel reacts with salts (e.g. NaCl) which are in the intake air, at the high temperatures of the combustion gases [2–5]. Due to the cooling (either internal or external) of the blades it is possible for the surface temperature to fall below the dew point of the sulfide vapor which then condenses on the blade surface. Film cooling is one of the methods used to cool turbine blades. There has been much experimental and analytical research in this field. Some examples are given in refs. [6–9].

The deposition of vapors on the blade surface is also a function of the mass transfer coefficient, as well as the temperature of the surface and the dew point of the vapor. The general aim of this experimental study is to determine the effects of injection on mass transfer. It is argued that (similar to film cooling) injection will decrease the mass transfer, thereby reduce the deposition rate and thickness on the surfaces resulting in decreased corrosion.

This paper presents measured mass transfer coefficients and effectiveness of a single row of holes (inclined 30° with the surface and inline with the main flow direction) in a zero pressure gradient flat plate turbulent boundary layer. There have been a few studies where both of these quantities were measured under the same flow conditions. In order to be able to calculate the mass (or heat) transfer to a film cooled surface, both of these quantities are necessary. Eriksen and Goldstein [10] and Liess [11] have reported results of similar measurements. The data collected will be compared with results of these studies.

STANTON NUMBER AND EFFECTIVENESS

The heat transfer film cooling effectiveness is given by [6]

$$\eta_t = \frac{T_{aw} - T_\infty}{T_j - T_\infty} \tag{1}$$

where T_{aw} is the adiabatic wall temperature, T_j is the temperature at the jet exit, and T_∞ is the temperature of the free stream.

In a similar manner a mass transfer effectiveness can be defined in terms of the mass fractions, which reduces to the following form if the total density is constant [6]

$$\eta_m = \frac{\rho_{iw} - \rho_\infty}{\rho_j - \rho_\infty} \tag{2}$$

where ρ is the density. According to the analogy between heat and mass transfer the two effectivenesses are equivalent if the Schmidt number is one [6].

†Presented at the International Gas Turbine Conference and Exhibit, Dusseldorf, West Germany, 8–12 June 1986.

NOMENCLATURE

C	arbitrary constant
D	diameter of jet
E	distance from virtual origin to naphthalene surface
H	boundary layer shape factor
h	mass transfer coefficient
M	blowing ratio
$\dot{m}$	mass transfer rate
P	distance between jets (pitch)
Pr	Prandtl number
p, q	constants in equation (10)
Re	Reynolds number
Sc	Schmidt number
St	Stanton number
T	temperature
U	velocity
u^+, y^+	boundary layer wall coordinates
x, y, z	boundary layer coordinates
x	distance from jet exit
x'	distance from boundary layer trip.

Greek symbols

α	angle between jet and surface
δ_1	displacement thickness
δ_2	momentum thickness
η	effectiveness
ρ	density.

Subscripts

aw	adiabatic wall
iw	impermeable wall
j	jet
m	mass transfer
t	heat transfer
∞	free stream.

The effectiveness may be expressed as a function of the following parameters [12]

$$\eta_m = \eta_m(Re, M, P/D, Sc, \alpha). \tag{3}$$

If the Reynolds number and geometry $(P/D, \alpha)$ of the flow are held constant they may be removed from this expression. Pedersen *et al.* [13] experimentally found that the Schmidt number has no effect on the effectiveness if the density ratio of the injected and the free stream gases was near one. Thus under these conditions, the effectiveness will be a function of the blowing ratio only. The effectiveness for a film cooled surface has been measured by placing a trace gas into the injected gas stream. Some examples of these studies are given by Andrews *et al.* [14], Goldstein *et al.* [15], Foster and Lampard [16] and others.

A mass transfer coefficient h_m, for a film cooled surface is defined as

$$\dot{m} = h_m(\rho_w - \rho_{iw}) \tag{4}$$

where $\dot{m}$ is the mass transfer per unit area, ρ_w is the density at the wall and, ρ_{iw} is the density at an impermeable wall with the same free stream conditions. This mass transfer coefficient is not a function of densities, but only a function of the flow field [6]. Combining equations (2) and (4) while eliminating ρ_{iw} gives

$$\dot{m} = h_m[(\rho_w - \rho_\infty) - \eta(\rho_j - \rho_\infty)]. \tag{5}$$

Once h_m and η_m are known for a given flow field, the mass transfer can be calculated from equation (5).

A mass transfer Stanton number is defined as

$$St_m = \frac{h_m}{U_\infty} \tag{6}$$

where U is the free stream velocity, the Stanton number is a function of the same variables that are shown in equation (3). Under the restrictions of constant geometry, Reynolds number and blowing ratio

$$St_m = C\,Sc^n \tag{7}$$

where C is a constant and n has a value of 0.4 [17]. In the final goal of this experimental project (effect of injection on vapor condensation) equation (5) will be used to calculate the mass transfer of water vapor to the wall. Condensation of water vapor will be used to model condensation of sodium sulfate on a film cooled turbine blade. Since the vapor has a Schmidt number different from either naphthalene or CO_2, equation (7) will be used to correct the Schmidt number effects.

EXPERIMENTAL APPARATUS AND METHODOLOGY

The experiments were performed in an open circuit subsonic wind tunnel with a free stream turbulence level of 0.3%. The boundary layer was fully turbulent and had a zero pressure gradient. All measurements were made under isothermal ambient conditions. A sketch of the wind tunnel and injection section is shown in Fig. 1. Detailed information on the experimental apparatus can be found in ref. [18]. The test section is 3.05 m long and 45.72 × 30.48 cm in cross section. The wind tunnel has an adjustable ceiling which allows for different pressure gradients to be set. It is made up of 16 sections of 15.24 cm wide plexiglas. The sections form an air tight surface, and each section could be adjusted independently.

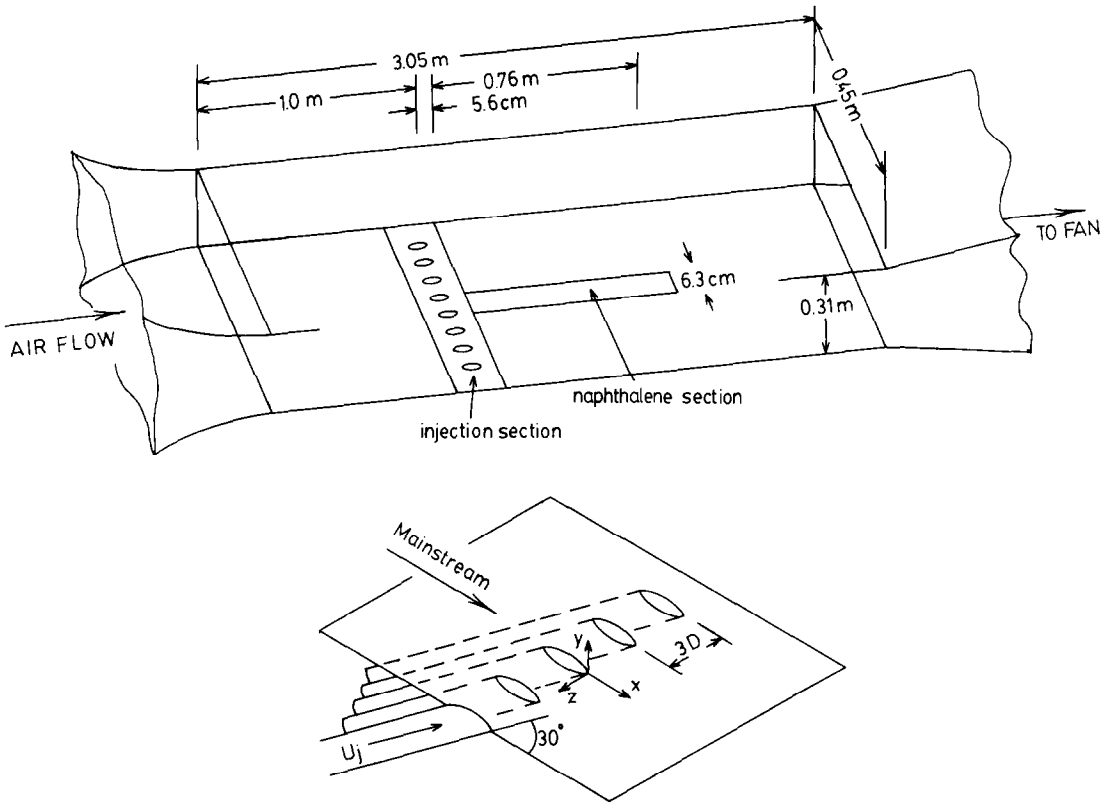

FIG. 1. Sketch of subsonic wind tunnel and injection section.

The injection section is located 1 m downstream from the nozzle exit. A boundary layer trip made of sandpaper 2 cm wide is located at the exit of the nozzle. The jets are aligned with the flow and are 30° with the horizontal. The exit section is stainless steel tubing with an inner diameter of 1.021 cm. The tubes pass through a stainless steel plate with a pitch-to-diameter ratio of 3.0. The tubes are 59 diameters long to ensure fully developed turbulent flow at the exit. The injection gas is building compressed air at 400 kPa. A trace gas (used in the measurement of the effectiveness) can be introduced into a mixing chamber. At the exit of the mixing chamber eight polyethylene tubes (0.953 cm o.d.) were connected to carry the air and trace gas to the injection jets. Each tube has a valve and flowmeter allowing the flow in each to be adjusted. The flow to the injection system is monitored by a calibrated rotometer and controlled by a single upstream metering valve.

Measurement of the mass transfer effectiveness

A trace gas (carbon dioxide) was injected into the secondary flow upstream in the manifold. A probe was constructed using two stainless steel capillary tubes soldered side by side. One of the tubes was used as a total pressure probe while the other as a sampling probe. The sampling tube was connected to a vial, which was then attached through a needle valve to a vacuum pump. The vacuum was increased until the pressure reading changed. The vacuum was then reduced slightly. This was done to ensure that the flow was not altered by the suction. The density gradient (first derivative with respect to y) at the wall is zero since the wall is impermeable. The boundary layer species transport equation evaluated at the wall requires the second derivative also to be zero. A third-order polynomial, which is the simplest curve that satisfies these conditions, is

$$\rho(y) = a + by^3. \tag{8}$$

Samples were taken at four locations above the wall. The first was as close to the wall as possible (0.127 mm), while the next three were at intervals of 0.07, 0.15, and 0.30 mm. Using the four data points, the values of a and b were determined using the method of least squares. The polynomial was then evaluated at the wall to determine ρ_{iw}, which was the value of 'a'. This method of measurement was chosen since the authors believe that it gives more reliable results than the alternative technique of measuring wall concentration through holes drilled at the wall. In this case, extraction of the sample introduces a normal velocity component at the wall, altering concentration distribution and rendering the wall no longer impermeable.

The concentration of the trace gas was measured using a Hewlett–Packard Model 700 Gas Chromatograph, which had a thermal conductivity detector. The concentration of CO_2 in the jets was approximately 25 times its ambient concentration of 314 p.p.m. In order to detect concentrations this low it was necessary

to amplify the signal. An Ectron Model 750 DL Differential Amplifier was used. It had a gain of 1000 and a 1 Hz, three pole Bessell filter. The density ratio between the jet and free stream was 1.015.

Measurement of the mass transfer coefficient

The mass transfer was measured using a naphthalene sublimation technique described in ref. [19]. A portion of the flat plate downstream of the injection section was replaced with naphthalene. A test section was constructed with a slot 6.35 cm wide and 76.2 cm long. This slot allowed a frame to be easily inserted and removed. The slot began 5.6 cm downstream from the centerline of the injection ports. The centerline of the frame was along the centerline of the wind tunnel. The frame consisted of four side walls, the top of which, along with the naphthalene formed a surface which filled the slot in the floor of the wind tunnel, resulting in an exposed napthalene surface 5.08 cm wide and 74.93 cm long.

The local height of the naphthalene surface was measured on the bed of a milling machine. The bed could be moved in the x- and z-direction and each was controlled by a lead screw with a dial marked in 0.0254 mm increments. The frame was mounted on the bed with two strong springs, which allowed it to be replaced in approximately the same location. The coordinates of 24 points on the surface of the frame were measured. A plane was fitted to these points using the method of least squares. This plane was then used as a reference for measuring the height of the naphthalene surface exposed to the flow field.

A total of 371 points on the naphthalene surface were measured. The data points were grouped more densely near the upstream end of the naphthalene. At each downstream location, 14 transverse measurements were obtained at 0.254 cm intervals. The first six rows in the downstream direction were spaced at 0.254 cm starting 6.18 cm downstream of the jets. The next eight rows were spaced at 0.635 cm intervals, followed by six rows at 1.27 cm intervals, followed by three rows at 2.54 cm intervals, followed by four rows at 5.08 cm intervals and the last four rows at 10.16 cm intervals. The last 12 rows had only 7 rather than 14 points across. The naphthalene surface was exposed to the flow field for 1 h. After exposure, the surface measurement procedure was repeated. The change in the height of the naphthalene surface was the total mass transfer.

The density of naphthalene at the wall was determined from the ideal gas equation of state. The partial pressure was calculated from an integrated form of the Clausius–Clapeyron equation. For naphthalene

$$\ln(P_v) = 34.26 - 8587.4/T \qquad (9)$$

where the pressure is in kPa and T is in Kelvin [20]. With the density of naphthalene in the free stream and jet being equal to zero, and the measured mass transfer, the mass transfer coefficient can be calculated from equation (5). The wind tunnel was not exhausted outside the building. However, the room has a volume of over 500 m^3 and all doors and windows were open for the duration of the tests. The room temperature variation was less than 1 °C during the duration of the tests. The total mass of naphthalene sublimated during the entire test divided by the volume of the rooms yields a ρ three orders of magnitude less than ρ_w. This allowed ρ to be assumed as zero.

RESULTS AND DISCUSSION

Wind tunnel qualification

All experiments were conducted with a free stream velocity of 21.0 $m\,s^{-1}$. Before the measurements of mass transfer and effectiveness, the wind tunnel qualification tests were made. This consisted of three parts. First the flow was shown to be two-dimensional. Second, the boundary layer profiles were shown to agree with non-dimensional turbulent boundary layer profiles presented in the literature. Third, the flow downstream of the injection was found to be periodic in the transverse direction, indicating correct adjustment of the individual flow rates in each jet.

Velocity profiles with no injection were measured with a total pressure probe. The static pressure was measured with taps mounted flush to the tunnel walls. Three velocity profiles were obtained at each of five streamwise measuring locations spaced at 20 cm intervals, starting at the nozzle exit. The three profiles at each downstream location were approximately 25% of the tunnel width apart in the transverse direction. When three profiles were plotted on the same graph they were seen to coincide within 2.1%. The shape factors ($H = \delta_1/\delta_2$) were calculated and were seen to be within 1.5% of the values predicted theoretically (using the one-seventh power law assumptions). The virtual origin was calculated and seen to be 7.25 cm before the boundary layer trip [18]. These results show the boundary layer to be two-dimensional and fully turbulent.

Several traverses were made at the exit of the jets without the main flow to check the uniformity of the flow through each jet. The traverses were made through the centerline of the jets 3.0 cm downstream and 1.5 cm above the surface. The velocity in the jets had three values 14.2, 17.8 and 26.12 $m\,s^{-1}$ which correspond to the jet velocities for blowing ratios of 0.4, 0.8, and 1.2. The maximum variation from the mean was less than 4.6%, indicating correct adjustment of the control value for each jet.

Mass transfer effectiveness

As a preliminary to the measurement of the effectiveness, several profiles of the density of CO_2 was measured through the boundary layer. Figure 2 shows the density (normalized in the same manner as the effectiveness) as a function of the distance from the wall. The data in Fig. 2 were obtained ten diameters downstream and along the centerline of the jet. At

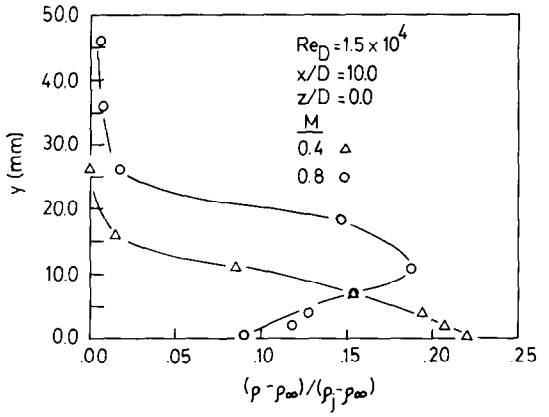

FIG. 2. Concentration profiles downstream of a row of film cooling holes.

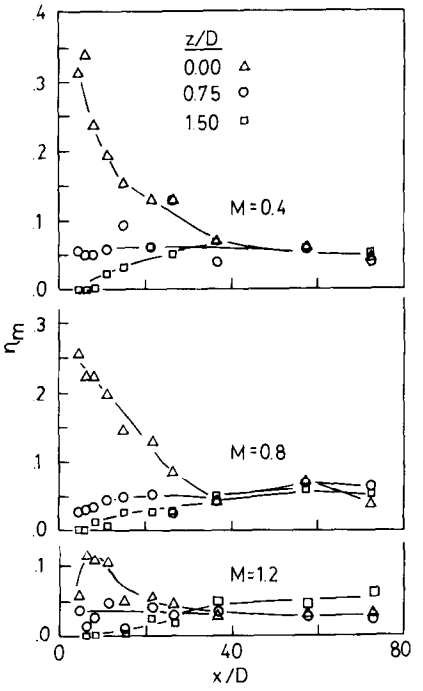

FIG. 3. Streamwise variation of effectiveness at three streamwise locations for different blowing ratios.

the blowing ratio of 0.4 the jet effluent remains low in the boundary layer and yielded an effectiveness of 0.23. At $M = 0.8$, the jet effluent penetrates higher into the boundary layer resulting in a lower effectiveness of 0.08.

The mass transfer effectiveness was measured at ten downstream locations. Five measurements were made in the transverse direction at each downstream location at intervals of 0.35 from the centerline of the jet. The effectiveness was measured at each point for each of the three blowing ratios.

Figure 3 shows the spanwise change of effectivenss at locations z/D of 0, 0.75, and 1.5 as a function of dimensionless distance from the jet exit (x/D) and the blowing ratio. The value of z is measured from the

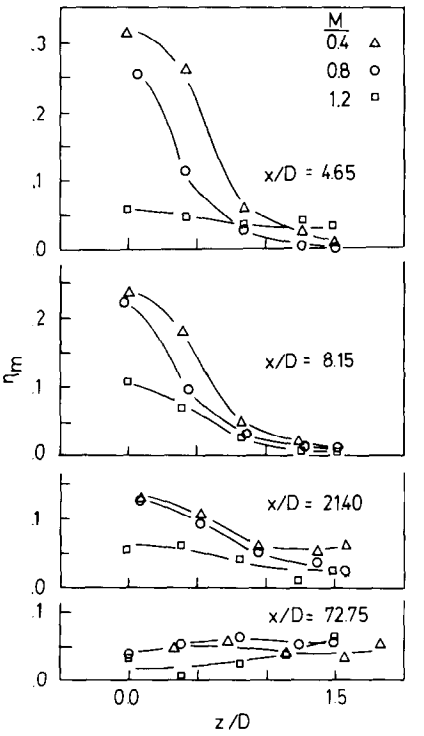

FIG. 4. Spanwise variations of effectiveness at three blowing ratios for four downstream locations.

centerline of the jet in the transverse direction. For $z/D = 0$, the effectiveness is at its maximum value nearest the jet ($x/D = 5.15$) for all the three blowing ratios. It then decreases in the downstream direction. For $z/D = 1.5$ (equidistance between the jets) the effectiveness is zero at $x/D = 5.15$ and increases with x/D due to jet coalescence. For $z/D = 0.75$ the effectiveness has a moderate value which increases slightly in the downstream direction.

Figure 4 shows the effectiveness for different distances downstream from the jets, at each blowing ratio. At 4.65 diameters from the jet, the effectiveness has a large variation in the z-direction for blowing ratios of 0.4 and 0.8. At a blowing ratio of 1.2, the effectiveness is almost constant but lower than the effectiveness for blowing ratios of 0.4 and 0.8 for all values of z/D. This is attributed to the increased mixing with the main flow at lower blowing ratios. This variation in the z-direction decreases until it disappeares downstream in the recovery region ($x/D = 20$). For $M = 0.4$, this spanwise dependence persists for about 50 hole diameters downstream. At the highest blowing ratio, the spanwise dependence is never as pronounced as for the lowest blowing, and disappears after about 25 hole diameters. For $M = 0.8$, there is a strong spanwise dependence near the jets but it disappears after about 35 diameters.

Figure 5(a) presents the spanwise-averaged effectiveness as a function of the blowing ratio at four downstream locations. The effectiveness is at a maximum for a blowing ratio between 0.4 and 0.8 for

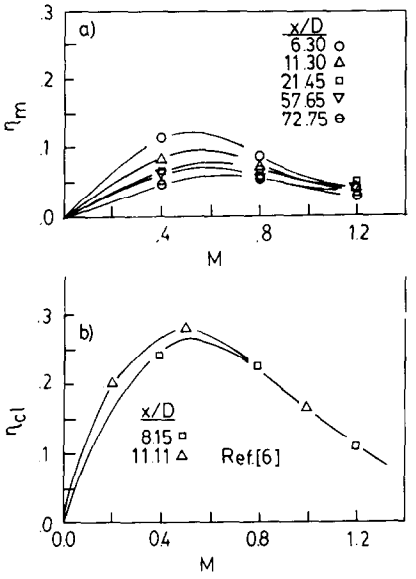

FIG. 5. (a) Variation of spanwise averaged effectiveness with blowing ratio at four downstream locations, (b) comparison of centerline effectiveness to that from ref. [6].

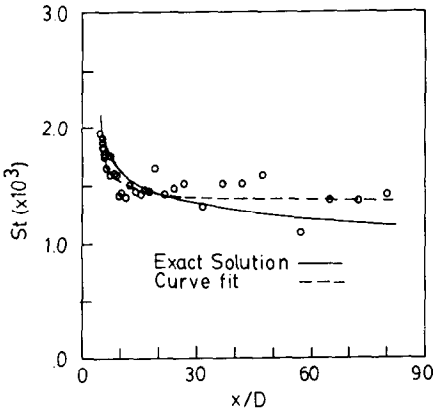

FIG. 6. Spanwise averaged Stanton number with no blowing as a function of distance from holes.

all but the last downstream location. At the last location, the effectiveness shows only a slight variation with the blowing ratio. This is consistent with previous findings [10, 11]. As a reference, the centerline effectiveness is compared to that from ref. [6] in Fig. 5(b). This data was collected at $x/D = 11.11$ and with an injection angle of 35°.

Mass transfer coefficient

The mass transfer coefficient was measured at 32 downstream locations for each of the three blowing ratios and with no blowing. At the first 20 locations, 14 measurements were made in the spanwise direction, while 7 were made at the last 12 downstream locations.

In the case of no blowing, plastic tape was placed over the jets to make the injection surface as smooth as possible. Figure 6 shows the mass transfer coefficient with no blowing as a function of x. The data were spanwise averaged as in ref. [21]. An exact

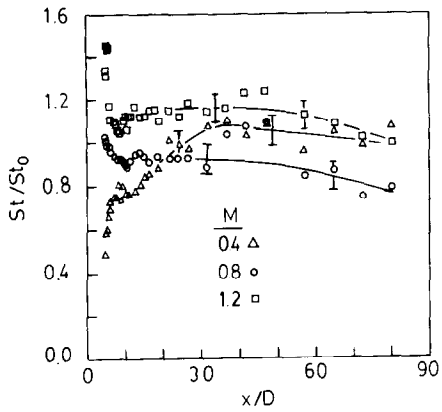

FIG. 7. Spanwise averaged Stanton number ratio as a function of distance from holes for three blowing ratios.

solution from ref. [22] for mass transfer with a step change in surface density has the form

$$St_m = C\,Re^p\left(1 - \left(\frac{E}{X'}\right)^{0.9}\right)^q \tag{10}$$

where C, p and q are constants, E is the starting length with no mass transfer and X' is the distance from the virtual origin. The Schmidt number effect is included in C. Using the constants in ref. [21] yields the dashed line. The data is within 15% of the exact solution, however the exact solution underpredicts the data at downstream locations and overpredicts in the region near the jets. The dashed line is a curve fit of the data with the same form as equation (10) where C, p and q were determined using the method of least squares. The dashed line in Fig. 6 was used to normalize the data for mass transfer with blowing. Figure 7 presents the results for the three blowing ratios. Again the data were averaged in the spanwise direction. An uncertainty analysis of the data was done following Moffat [23]. The calculated uncertainty was approximately ± 9% of the measured value at each point. Eriksen and Goldstein [10] reported a spanwise variation of approximately 10–20%. For this reason, spanwise variation in the Stanton numbers are not reported.

In the region behind the jets the mass transfer coefficient at a blowing ratio of 1.2 was increased by 40%. It decreased in the downstream direction, and was higher than that of the other two blowing ratios over the entire test section. The lowest blowing reduced the mass transfer coefficient by 35% just behind the jets, but it increased in the downstream direction. The intermediate blowing ratio (0.8) increased the mass transfer coefficient by about 5% behind the jets, however it decreased downstream to a value below that for the lowest blowing ratio. This indicates that the optimum mass transfer coefficient is at a blowing ratio greater than 0.4.

Figure 8 presents the mass transfer coefficient as a function of the blowing ratio at four downstream

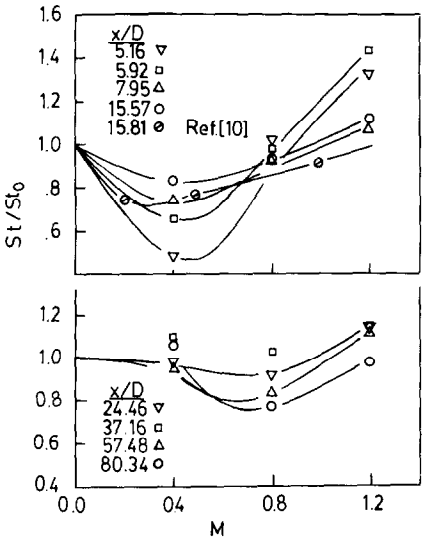

FIG. 8. Variation of normalized Stanton number with the blowing ratio at eight downstream locations.

locations. The figure indicates that the blowing ratio with the lowest mass transfer coefficient is between 0.4 and 0.8 for all locations except very close to the jets. Data from ref. [10] at $x/D = 15.81$ is also plotted as a reference. This data was taken at a higher Re_D and the angle of injection was 35°.

Summary

These results show that at the high blowing ratio of 1.2 the mass transfer coefficient was increased and the effectiveness was lower than other blowing rates. This combination results in high mass (or heat) transfer to the surface. At the lowest blowing ratio (0.9), the mass transfer coefficient was reduced and the effectiveness was high, which reduces the heat or mass transfer. At the intermediate blowing ratio the effectiveness is slightly lower than for $M = 0.4$, however the mass transfer coefficient is smaller in the far recovery regions ($x/D \geq 40$) than either the high or low blowing. This indicates that the optimum blowing ratio is between 0.4 and 0.8. Previous researchers' (refs. [10, 11] and others) work has indicated that the optimum blowing for film cooling is about 0.5 which is consistent with the results presented here.

CONCLUSIONS

(1) The mass transfer coefficient and effectiveness were measured downstream of one row of holes inclined 30° with the horizontal in an isothermal turbulent boundary layer on a flat plate. The data were collected at blowing ratios of 0.4, 0.8 and 1.2.

(2) The mass transfer coefficient obtained had a minimum for a blowing ratio between 0.4 and 0.8.

(3) The effectiveness was seen to have a maximum at a blowing ratio between 0.4 and 0.8.

(4) In the region near the jets the effectiveness was highest for the low blowing ratio and lowest for the high blowing ratio whereas the normalized mass transfer coefficient had its largest value at the high blowing ratio and a minimum at the low blowing ratio.

(5) In the far recovery region, ($x/D \geq 40$) the effectiveness showed only slight dependence on the blowing ratio. The largest mass transfer coefficient occurred with high blowing ratios, but the intermediate blowing ratio had the lowest mass transfer coefficient.

(6) Using these experimentally measured values a general mass transfer equation based on the surface and free stream densities is derived (equation (5)). This general equation can be used on a surface with the same flow field for a general mass (or heat) transfer problem.

Acknowledgement—Support for this work from the National Science Foundation under NSF Research Initiation Grant MEA-8307153 is gratefully acknowledged. Also acknowledged is a Research Initiation Grant from the College of Engineering of Pennsylvania State University.

REFERENCES

1. A. B. Hart, J. W. Saxton, C. G. Stevens and D. Judy, Deposition of sodium compounds under gas turbine conditions. *In High Temperature Alloys for Gas Turbines* (edited by Coutsouradis, Felix, Fischmesiter, Habraken, Lindblom and Speidel), pp. 81–107. Applied Science, London (1979).
2. D. Rosner, K. Seshadri, M. Fernandez, G. C. Fryburg, F. J. Kohl, C. A. Sterns and G. J. Santoro, Transport, thermodynamic and kinetic aspects of salt/ash deposition rates from combustion gases, *Proceedings of 10th Material Research Symposium: Char. of High Temperature Vapors*. U.S. Government Printing Office (1979).
3. D. E. Rosner and M. Fernandez, Recent advances in the theory of salt/ash deposition in combustion systems, *Proceedings of DOE–EPRI Conf. on Adv. Materials/ Alternate Fuel Engines* (1979).
4. D. E. Rosner, Bor-Kuan Chen, G. C. Fryberg and F. J. Kohl, Chemically frozen multicomponent boundary layer theory of salt and/or ash deposition rates from combustion gases, *Combust. Sci. Technol.* **20**, 87–106 (1979).
5. C.A. Stearns, F. J. Kohl and D. E. Rosner, Combustion system processes leading to corrosive deposits, DOE/ NASA/2593–27 (1981).
6. R. J. Goldstein, Film cooling, *Advances in Heat Transfer* (edited by J. P. Hartnett and T. Irvine, Jr.), Vol. 7, pp. 321–379 (1971).
7. R. J. Goldstein, E. R. G. Eckert and J. W. Ramsey, Film cooling with injection through holes: adiabatic wall temperatures downstream of a circular hole, *Trans. Am. Soc. mech. Engrs, J. Engng Power* 384–395 (October 1968).
8. N. Hay, D. Lampard and C. L. Saluja, Effects of cooling films on the heat transfer coefficient on a flat plate with zero mainstream pressure gradient, ASME Paper 84-GT-40 (1984).
9. W. O. Afejuku, N. Hay and D. Lampard, Measured coolant distributions downstream of single and double rows of film cooling holes, ASME Paper 82-GT-144 (1982).
10. V. L. Eriksen and R. L. Goldstein, Heat transfer and film cooling following injection through inclined circular

tubes, *Trans. Am. Soc. mech. Engrs, J. Heat Transfer* **96,** 239–245 (1974).
11. C. Liess, Experimental investigation of film cooling with ejection from a row of holes for the application to gas turbine blades, ASME Paper 74-GT-5 (1974).
12. M. E. Crawford, W. M. Kays and R. J. Moffatt, Heat transfer to a full-coverage surface with 30 degree slant hole injection, NASA CR-2786.
13. D. R. Pedersen, E. R. G. Eckert and R. L. Goldstein, Film cooling with large density differences between the mainstream and the secondary fluid measured by the heat-mass transfer analogy, *Trans. Am. Soc. mech. Engrs, J. Heat Transfer* **99,** 620–627 (1977).
14. G. E. Andrews, M. L. Gupta and M. C. Mkpadi, Full coverage discrete hole wall cooling: cooling effectiveness, ASME Paper 84-GT-212 (1984).
15. R. L. Goldstein, E. R. G. Eckert and F. Burggraf, Effect of hole geometry and density on three-dimensional film cooling, *Int. J. Heat Mass Transfer* **17,** 595–607 (1974).
16. N.W. Foster and D. Lampard, The flow and film cooling effectiveness following injection through a row of holes, *Trans. Am. Soc. mech. Engrs, J. Engng Power* **102,** 584–588 (1980).
17. R. J. Goldstein and J. R. Taylor, Mass transfer in the neighborhood of jets entering a cross flow, *J. Heat Transfer* **104,** 715–721 (1982).
18. W. P. Webster, Condensation in the recovery region of a film cooled, isothermal, flat plate, Ph.D. thesis, The Pennsylvania State University, University Park, PA 16802 (1986).
19. H. H. Sogin, Sublimation from disks to air streams flowing normal to their surfaces, *Trans. Am. Soc. mech. Engrs, J. Heat Transfer* 61–69 (January 1958).
20. F. E. M. Saboya and E. M. Sparrow, Local and average transfer coefficients of one-row plate fin and tube heat exchanger configurations, *Trans. Am. Soc. mech. Engrs, J. Heat Transfer* 265–272 (August 1974).
21. S. Yavuzkurt, R. J. Moffat and W. M. Kays, Full-coverage film cooling. Part 1. Three-dimensional measurements of turbulence structure, *J. Fluid. Mech.* **101,** 29–158 (1980).
22. W. M. Kays and M. E. Crawford, *Convective Heat and Mass Transfer*. McGraw-Hill, New York (1980).
23. R. J. Moffat, Contributions to the theory of single-sample uncertainty analysis, *Trans. Am. Soc. mech. Engrs, J. Fluids Engng* **104,** 250 (June 1982).

MESURE DU COEFFICIENT DE TRANSFERT MASSIQUE ET DE L'EFFICACITE DANS LA REGION DE RECUPERATION D'UNE SURFACE REFROIDIE PAR UN FILM

Résumé—Les coefficients de transfert massique et l'efficacité du film réfrigérant sont mesurés en aval d'une rangée unique de trous (région de récupération) inclinée à 30° par rapport à la surface et en ligne avec l'écoulement principal à couche limite turbulente. Les coefficients de transfert massique sont mesurés en utilisant la technique de sublimation du naphtalène. L'efficacité est déterminée à l'aide de l'injection d'une trace de gaz dans l'écoulement secondaire et en mesurant sa concentration à la paroi imperméable. Des expériences sont faites dans une couche limite subsonique turbulente avec gradient de pression nul, sous des conditions isothermes, pour trois rapports de soufflage (U_j/U_∞): 0,4, 0,8 et 1,2. Les données sont collectées dans la région entre 7 et 80 fois le diamètre du jet en aval de la zone d'injection. On dérive une équation générale du transfert de masse et on présente une discussion des données. Il semble que cette étude et l'une des très rares dans lesquelles on mesure ensemble les deux variables sur la même surface et dans un large domaine de la région de récupération.

MESSUNGEN DES STOFFÜBERGANGSKOEFFIZIENTEN UND DER WIRKSAMKEIT IN DER RECOVERY-REGION EINER FILMGEKÜHLTEN OBERFLÄCHE

Zusammenfassung—Es wurden Stoffübergangskoeffizienten und Wirksamkeit der Filmkühlung stromabwärts von einer Reihe von Bohrungen (Recovery-Region) gemessen, welche bei einer Neigung von 30° in Richtung der turbulenten Grenzschichtströmung in die Oberfläche eingebracht waren. Die Stoffübergangskoeffizienten wurden unter Benutzung einer Naphthalin-Sublimationstechnik gemessen. Die Wirksamkeit wurde bestimmt durch das Einblasen eines Markierungsgases in die Sekundärströmung und durch Messung seiner Konzentration an der undurchlässigen Wand. Ausgeführt wurden die Experimente in einer druckgradientfreien turbulenten Grenzschicht im Unterschallbereich bei isothermen Bedingungen mit drei Einblasverhältnissen (U_j/U_∞): 0,4, 0,8 und 1,2. Die Daten wurden in einem Bereich von 7 bis 80 Düsendurchmesser stromabwärts von der Einblasstelle aufgenommen. Aus den unter denselben Strömungsbedingungen aufgenommenen Werten der Stoffübergangskoeffizienten und der Wirksamkeit wurde eine allgemeine Stoffübergangsgleichung abgeleitet. Diese Arbeit beinhaltet umfassende Daten und deren Erörterung; sie ist wohl eine der wenigen Untersuchungen, bei welcher beide Größen an derselben Oberfläche und in einem weiten Gebiet des Recovery-Bereichs gemessen wurden.

ИЗМЕРЕНИЯ КОЭФФИЦИЕНТА МАССОПЕРЕНОСА И ЭФФЕКТИВНОСТИ ПЛЕНОЧНОГО ОХЛАЖДЕНИЯ В ОБЛАСТИ ВОССТАНОВЛЕНИЯ

Аннотация—Коэффициенты массопереноса и эффективность пленочного охлаждения измеряются за одним рядом отверстий (область восстановления), расположенных под углом 30° к поверхности и параллельно основному течению турбулентного пограничного слоя. Коэффициенты массопереноса измеряются с помощью методики, использующей процесс испарения нафталина. Эффективность определяется через ввод газа-индикатора во вторичное течение и измерение его концентрации у проницаемой стенки. Эксперименты проводились в дозвуковом турбулентном пограничном слое с нулевым градиентом давления при изотермических условиях с тремя отношениями вдува (U_j/U_∞): 0,4; 0,8 и 1,2. Результаты получены на расстояниях от 7 до 80 диаметров струи от местоположения вдува. Из данных по коэффициентам массопереноса и эффективности, полученных при одних и тех же условиях течения, выведено основное уравнение по массопереносу. Представлены расширенные данные и их обсуждение; полагается, что данная работа является одной из немногих, в которых обе переменные измеряются на одной и той же поверхности и в большой по площади области восстановления.